Preparation of water-dispersible TiO_2 nanoparticles

Shi-Zhao Kang, Dieer Yin, Xiangqing Li, Qiang Zhang, Jin Mu

School of Chemical and Environmental Engineering, Shanghai Institute of Technology, 100 Haiquan Road, Shanghai 201418, People's Republic of China
E-mail: kangsz@sit.edu.cn

Published in Micro & Nano Letters; Received on 30th May 2014; Revised on 30th September 2014; Accepted on 21st October 2014

Water-dispersible TiO_2 nanoparticles with narrow size distribution and good crystallinity were synthesised in a solvothermal process using lactic acid as the capping agent. X-ray diffraction, transmission electron microscopy and nitrogen adsorption–desorption isotherm were used to characterise the products. Meanwhile, the dispersion behaviour of the as-prepared TiO_2 nanoparticles was investigated. The as-prepared powder can be easily redispersed in water to form a stable solution-like suspension with a concentration of 60 mg·ml^{-1}. Moreover, the dispersion mechanism was also preliminarily discussed, suggesting that the excellent dispersibility of the as-prepared TiO_2 nanoparticles is probably because of electrostatic repulsion from lactic acid molecules covalently linked to TiO_2 nanoparticles.

1. Introduction: During the past decades, TiO_2 nanoparticles have been a focus of research because of their potential applications in photocatalysts [1], solar cells [2], antibacterial materials [3], lithium batteries [4], sensors [5] and so on. However, it was recently found that the use of dry TiO_2 nanoparticles would cause some potential hazards to health [6]. As a result, it is necessary to develop some techniques which minimise such health hazards.

Compared with the dry process, the wet process, which has been regarded as a preferable handling technology of nanometre-sized particles, can reduce harm from nanoparticles caused by respiratory intake. Moreover, it is essential for various applications of TiO_2 nanoparticles, such as the fabrication of high-quality films, to distribute the nanoparticles in an appropriate solvent for homogeneous and stable concentrated dispersion [7]. Therefore, the stable dispersion of TiO_2 nanoparticles in liquids has received extensive attention, and a lot of effective preparation methods have been developed. The reported methods used for the preparation of stable dispersions of TiO_2 nanoparticles fall broadly into three categories. The first is pH adjustment [8]. The second is surface modification using surfactants, polymers, small molecules and so on. For example, Veronovski *et al.* [9] prepared a stable colloidal dispersion of TiO_2 nanoparticles (P25) employing cation Gemini surfactant as the dispersant. The third method is ultrasonic vibration [6]. Among these methods, surface modification using small molecules combined with ultrasonication would be promising from the viewpoint of practical applications because of the relatively low cost. However, the attractive interaction between nanoparticles in dispersion is very strong, so the dispersion is often unsatisfactory when small molecules are used as dispersant. Particularly, the stability of dispersion is poor. Thus, it is still desirable to improve the stability of concentrated aqueous suspensions when using small molecules as dispersant. Poly(L-lactic acid) (PLA) is a biodegradable polymer. A lot of studies concerning PLA-based nanocomposites have been reported. The previous results show that TiO_2 nanoparticles can be uniformly dispersed in PLA matrices [10], and the PLA-grafted TiO_2 nanoparticles can exhibit improved dispersion compared with bare TiO_2 nanoparticles [11]. Therefore, we can deduce that water-dispersible TiO_2 nanoparticles could be prepared using lactic acid as the capping agent, and the as-prepared TiO_2 nanoparticles can be dispersed in water to form a stable colloidal dispersion. Unfortunately, it is still unclear whether or not the water-dispersible TiO_2 nanoparticles can be prepared using lactic acid as the capping agent.

On the other hand, there is a great demand for transparent TiO_2 films in some applications, such as the window or reflector coating of photovoltaic devices, which need to use nanoparticles with sizes below 50 nm. In addition, the previous results indicate that high-quality films can be simply fabricated using nanocrystals with a sub-5 nm diameter [12]. Therefore, it is worthwhile to synthesise TiO_2 nanoparticles with a sub-5 nm diameter which can be well dispersed in water for the application of TiO_2 in the field of photovoltaic devices.

In this reported work, TiO_2 nanoparticles with sub-5 nm diameter were synthesised in a solvothermal process using lactic acid as the capping agent. Meanwhile, their dispersion behaviour in water was explored. The dispersion mechanism is preliminarily discussed. Lastly, the photocatalytic behaviour of the as-prepared TiO_2 nanoparticles was examined to check their potential application.

2. Experimental: Commercially available TiO_2 nanoparticles (P25) were purchased from the Degussa AG Company (Germany). Titanium tert-butoxide (TBT), ethanol, and lactic acid were commercially available and used as received. Deionised water was used as the solvent. In a typical procedure, lactic acid (1 ml) and ammonium acetate (0.5 g) were in turn added into a beaker containing ethanol (7.5 ml) at room temperature under stirring. Meanwhile, the ethanol solution of TBT was prepared by adding TBT (0.75 ml) to ethanol (10 ml) under stirring. After the TBT solution was poured into a 50 ml Teflon-lined stainless-steel autoclave, the solution of lactic acid and ammonium acetate was added dropwise into the TBT solution followed by another stirring for 30 min. Subsequently, the autoclave was sealed and kept at 180°C for 18 h. After the autoclave was cooled down to room temperature, the precipitate was collected by centrifugation and washed three times with ethanol. Finally, the white product was dried in vacuum at 60°C for 12 h. For comparison, other TiO_2 nanoparticles were prepared without the addition of lactic acid. The TiO_2 nanoparticles prepared in the presence of lactic acid are abbreviated to **T-1**, while the TiO_2 nanoparticles prepared in the absence of lactic acid are abbreviated to **T-2**.

Powder X-ray diffraction (XRD) analysis was carried out using a PANalytical Xpert Pro MRD X-ray diffractometer (The Netherlands) using Cu Kα radiation at a scan rate of 1° min^{-1}. The samples for XRD were supported on glass substrates. The transmission electron microscopy (TEM) images and the high-resolution TEM (HRTEM) image were taken on a JEM-1400 transmission electron microscope (JEOL, Japan). The as-prepared TiO_2 powder was dispersed in ethanol by means of sonication. Then, the samples for the TEM characterisation were prepared by depositing a droplet of the dispersion on a Formvar/Carbon copper grid.

doi: 10.1049/mnl.2014.0305

The UV–vis spectra of the suspensions were measured with a Shimadzu UV-3600 spectrophotometer (Japan). N_2 adsorption and desorption isotherms were measured on a Micrometrics ASAP-2020 nitrogen adsorption apparatus (USA). The Fourier transform infrared (FTIR) spectra were recorded with a Nicolet 6700 FTIR spectrometer (USA). The samples for the FTIR spectra were prepared by mixing the TiO_2 nanoparticles with KBr and forming a pellet. The electrophoresis mobility of the nanoparticles was determined at 25°C using a Malvern Zeta Sizer Nano ZS90 instrument (UK), and their zeta potential was calculated by the Dispersion Technology Software provided by Malvern.

The photocatalytic experiments were carried out in a reactor containing the catalyst (1 mg ml^{-1}) and methyl orange (MO) aqueous solution (30 ml, 5×10^{-5} mol l^{-1}). A 350 W high-pressure Hg lamp was used as the UV radiation source. The distance between the lamp and the reactor was 20 cm. The catalyst was suspended in the dark for 30 min to reach adsorption equilibrium prior to irradiation. After irradiation, the residual concentration of MO was monitored by measuring the absorbance at 464 nm. The photocatalytic degradation efficiency of MO was calculated according to the following equation

$$\text{Efficiency}(\%) = (A_0 - A)/A_0 \times 100\% \quad (1)$$

where A_0 represents the absorbance of MO solution after being stirred in the dark for 30 min and A is the absorbance after irradiation.

3. Results and discussion: Fig. 1 shows the XRD patterns of **T-1** and P25. As can be seen from Fig. 1*a*, there exist 11 strong peaks at 25.3°, 37.3°, 37.8°, 38.6°, 48.1°, 53.9°, 55.1°, 62.7°, 68.9°, 70.4° and 75.2°, corresponding to the (101), (103), (004), (112), (200), (105), (211), (204), (116), (220) and (215) planes of the anatase TiO_2, respectively (JCPDS File No. 21-1272) [13, 14]. Moreover, no diffraction peaks from crystalline impurities are found. These phenomena show that the anatase TiO_2 with high phase-purity and good crystallinity were prepared in the process reported.

To substantiate the formation of nanoparticles, the morphology of the sample was observed using TEM (Fig. 2). From Fig. 2*a*, we clearly observe the irregular TiO_2 nanoparticles with a mean diameter of approximately 2.0 nm. In addition, any obvious agglomeration is not found. The size distribution of TiO_2 nanoparticles is narrow. The diameter of more than 85% particles is in the range of 1.5–3.0 nm. In the HRTEM image of **T-1**, some lattice fringes are clearly recorded, suggesting that **T-1** has good crystallinity. However, the average crystallite size of the sample calculated according to Scherrer's equation is 33 nm. One possible explanation is that the obtained powder consists of the TiO_2 nanoparticle aggregates. When the TiO_2 powder is dispersed in a liquid, these

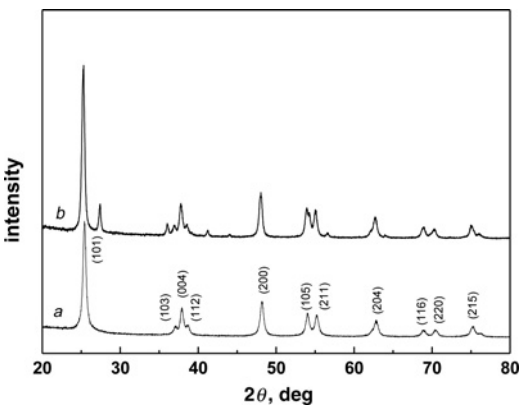

Figure 1 *XRD patterns*
a **T-1**; *b* P25

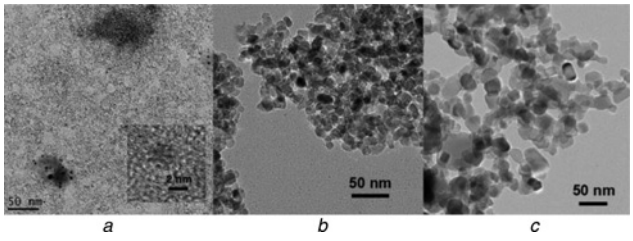

Figure 2 *TEM images*
a **T-1**
b **T-2**
c P25
Insert of (Fig. 1*a*): HRTEM image of **T-1**

TiO_2 nanoparticle aggregates become individual nanoparticles. Furthermore, it can be observed that both **T-2** (Fig. 2*b*) and P25 (Fig. 2*c*) are much bigger than **T-1**. Also, we can find obvious agglomeration from Figs. 2*b* and *c*. On the basis of these results, it can be deduced that the individual anatase TiO_2 nanoparticles with a sub-5 nm diameter can be obtained according to the procedure described above, implying that the as-prepared TiO_2 nanoparticles may possess a large specific surface area. Therein, lactic acid plays an important role. The specific surface area of **T-1** is 116 m^2 g^{-1}, which is much larger than that of P25 (50 m^2 g^{-1}) [15].

The dispersion behaviour of **T-1** was investigated by dispersing it in deionised water and comparing with that of P25. Fig. 3 shows the photographs of aqueous dispersions of **T-1** and P25. It can be found that **T-1** can be dispersed well in water under sonication. Even if the content of TiO_2 nanoparticles is up to 60 mg ml^{-1}, TiO_2 nanoparticles are dispersed in water to form a translucent solution-like dispersion. In contrast, we can only obtain a white milky suspension of P25 although its content is lower (1 mg ml^{-1}). In addition, the dispersion of **T-1** is very stable. After 24 days, the dispersion of TiO_2 nanoparticles (1 mg ml^{-1}) is still transparent and no precipitation is observed at the bottom of the vessel (Fig. 4*c*). After 34 days of storage, only a little precipitation can be found at the bottom of the vessel (Fig. 4*d*). When the content of TiO_2 nanoparticles increases up to 60 mg ml^{-1}, the solution-like dispersion can also keep transparent after 5 days. In contrast, the precipitation of P25 begins only after 8 h (Fig. 4*e*). These results indicate that the as-prepared TiO_2 nanoparticles possess dramatic dispersibility in water, which is very encouraging for potential applications.

Fig. 5*a* shows the UV–vis spectrum of the dispersion of **T-1** (1 mg ml^{-1}). As can be seen from Fig. 5*a*, the dispersion shows an optical threshold at 360 nm, which should be ascribed to a charge-transfer process from the valence band to the conduction

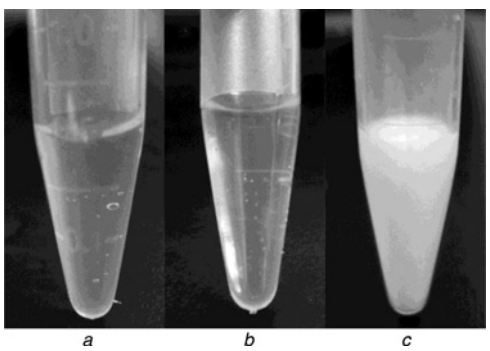

Figure 3 *Photographs of aqueous dispersions of* ***T-1***
a 1 mg ml^{-1}
b 60 mg ml^{-1}
P25
c 1 mg ml^{-1}

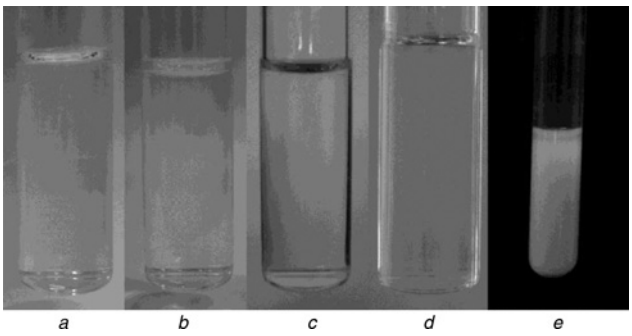

Figure 4 *Photographs of aqueous dispersions of* ***T-1*** *(1 mg ml^{-1})*
a After 1 day
b 15 days
c 24 days
d 34 days as well as the aqueous dispersion of P25 (1 mg ml^{-1})
e After 8 h

band of the TiO_2 nanoparticles. Moreover, the absorption band edge of **T-1** obviously blueshifts in comparison with those of **T-2** (Fig. 5*b*) and P25 (Fig. 5*c*). According to the formula reported by Ghosh *et al.* [16], the energy gap (E_g) value of **T-1** dispersed in water is estimated to be approximately 3.44 eV. Clearly, the bandgap of the TiO_2 nanoparticles synthesised here is obviously wider than that of the bulk anatase TiO_2 (3.2 eV) [17]. This phenomenon ought to be ascribed to the quantum confinement effect of small particles. According to the results reported previously [18], the dependence of particle size on absorption onset can be shown as follows

$$E* \simeq E_g + h^2\pi^2/2R^2\left(1/m_e^* + 1/m_h^*\right) - 1.8e^2/\varepsilon R \qquad (2)$$

where E_g is the bandgap of the bulk anatase TiO_2, h is the Plank's constant, m_e^* is the effective mass of the electron, m_h^* is the effective mass of the hole, e is the charge of the electron and ε is the dielectric permittivity of TiO_2. If we assume $\varepsilon = 184$, $m_e^* = 9\ m_e$ and $m_h^* = 2\ m_e$ in the light of [18, 19], it can be calculated that the average size of TiO_2 nanoparticles in the dispersion is about 2.4 nm. This result is almost the same as that from the TEM image, implying that no aggregation took place when **T-1** is dispersed in water. Furthermore, the absorption band of **T-1** is steep. The steep shape of the edge further shows that the as-prepared TiO_2 nanoparticles are dispersed well in water. Thus, it can be seen that the TiO_2 nanoparticles synthesised here are water-dispersible, and can be present in water as individual particles.

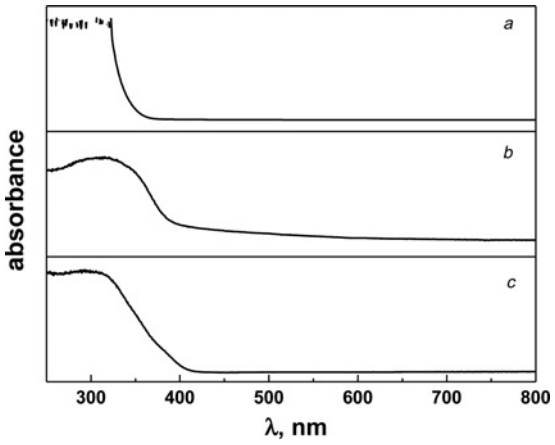

Figure 5 *UV–vis spectra of aqueous dispersions*
a **T-1**; *b* **T-2**; *c* P25 (1 mg ml^{-1})

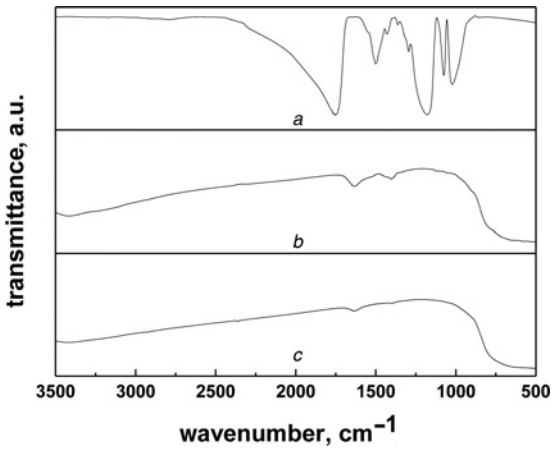

Figure 6 *FTIR spectra*
a **T-1**; *b* **T-2**; *c* P25

To understand the dispersion behaviour of **T-1**, the FTIR spectrum and zeta potential were measured. Fig. 6 shows the FTIR spectra of **T-1**, **T-2** and P25. In the case of **T-1**, the band at 1755 cm^{-1} corresponds to the C=O stretching vibration of polylactic acid [20, 21]. The band at 1430 cm^{-1} is assigned to the $-CH_3$ asymmetric bending vibration of polylactic acid, the band at 1362 cm^{-1} to the $-CH_3$ symmetric bending vibration, the band at 1294 cm^{-1} to the –C–O–C– stretching vibration, the band at 1178 cm^{-1} to the –C–O–C– asymmetric stretching vibration, the band at 1074 cm^{-1} to the –C–O–C– symmetric stretching vibration and the band at 1023 cm^{-1} to the C–C stretching vibration [21]. Compared with the bands of semi-crystalline polylactic acid reported in the literature [21], the bands assigned to $-CH_3$, –C–O–C and C–C groups obviously redshift while the band at 1755 cm^{-1} is attributed to the C=O stretching vibration slightly redshifts by 5 cm^{-1}. These results indicate that the as-prepared TiO_2 nanoparticles are coated with polylactic acid. The C=O groups of polylactic acid are oriented towards water to form a hydrophilic layer on the TiO_2 nanoparticles, which leads to the excellent dispersibility in water.

From Fig. 6, it can be also seen that there exists a band at 1503 cm^{-1} not belonging to polylactic acid. This band may be attributed to COO^- asymmetric stretching vibration, implying that surface carboxylate groups are present on the surface of the TiO_2 nanoparticles [21]. The results of zeta potential measurement also confirm this speculation. The zeta potential of **T-1** is −50 mV in a neutral solution. Therefore, it can be deduced that there exists strong electrostatic repulsion between TiO_2 nanoparticles, which causes high stability of dispersion.

Moreover, compared with the band assigned to the COO^- asymmetric stretching vibration of lactate (1585 cm^{-1}) [21], the band above redshifts by 82 cm^{-1}. This phenomenon may be ascribed to the interaction between the surface Lewis acid (Ti^{4+}) and the carbonyl oxygen atom [21]. On the basis of these results, a possible mechanism is suggested. At first, small TiO_2 nanoparticles are formed. Meanwhile, lactic acid would polymerise to form oligomers [22]. The oligomer of lactic acid is adsorbed onto the surface steps and defects of TiO_2 nanoparticles so as to block these growing points [23]. As a result, TiO_2 nanoparticles with a sub-5 nm diameter are prepared. Next, dissociation at some C–O bonds in the oligomer chains occurs on the surface of TiO_2 nanoparticles. These molecular fragments can react with the surface hydroxyl groups of TiO_2 nanoparticles to form the surface structure containing 2-oxy-propionic acid ($CH_3CH(O)COOH$, Fig. 7) [21]. Then, the oligomer chains extend on the surface of TiO_2 nanoparticles and the C=O groups are oriented towards water induced by hydrophobic interaction and the polarity of the carboxylate groups. Finally, the

doi: 10.1049/mnl.2014.0305

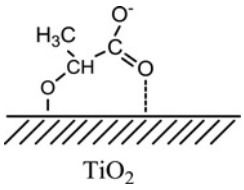

Figure 7 *Schematic diagram of the surface structure of as-prepared TiO_2 nanoparticles*

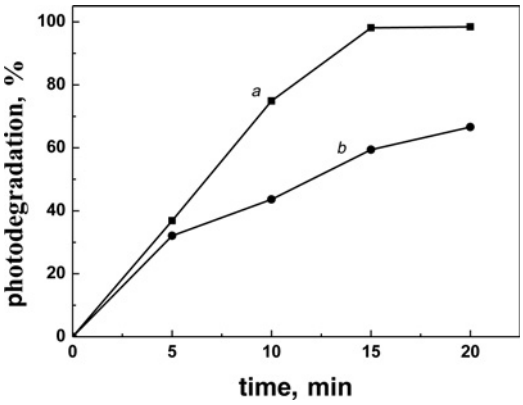

Figure 8 *Kinetic curves of MO (5×10^{-5} mol l^{-1}) degradation under UV irradiation in the presence of* ***T-1*** *and P25*
a **T-1**; *b* P25

water-dispersible TiO_2 nanoparticles are formed. Therein, the excellent dispersibility of TiO_2 nanoparticles mainly originates from the surface structure containing 2-oxy-propionic acid.

To check the potential use of **T-1**, its photocatalytic behaviour was examined. Fig. 8*a* shows the relationship of irradiation time and the degradation ratio of MO. From Fig. 8*a*, it can be observed that the solution is decolourised completely after 20 min irradiation in the presence of **T-1** (ca. 98% of degradation ratio of MO). Moreover, the photocatalytic activity of **T-1** is obviously higher than that of P25 (Fig. 8*b*). These results indicate that **T-1** possesses very high photocatalytic activity for the degradation of dye in water, which makes it very attractive for practical applications.

4. Conclusion: Water-dispersible TiO_2 nanoparticles can be prepared via a simple solvothermal method using lactic acid as a capping agent. This route does not involve any surfactants. It is simple, fast, 'green', and has potential for large-scale production. Moreover, the TiO_2 nanoparticles obtained possess excellent dispersibility in water, which may be applied widely in the fields of photovoltaic devices, sensors, antibacterial materials and so on. Further research efforts are currently being undertaken.

5. Acknowledgments: This work was supported by the Key Project of Science and Technology Innovation of the Shanghai Education Commission (no. 13ZZ135) and the Open Project of the State Key Laboratory of Supramolecular Structure and Materials (no. sklssm201424).

6 References

[1] Wesarg F., Schlott F., Grabow J., *ET AL.*: 'In situ synthesis of photocatalytically active hybrids consisting of bacterial nanocellulose and anatase nanoparticles', *Langmuir*, 2012, **28**, pp. 13518–13525

[2] He J.-A., Mosurkal R., Samuelson L.A., Li L., Kumar J.: 'Dye-sensitized solar cell fabricated by electrostatic layer-by-layer assembly of amphoteric TiO_2 nanoparticles', *Langmuir*, 2003, **19**, pp. 2169–2174

[3] Guin D., Manorama S.V., Latha J.N.L., Singh S.: 'Photoreduction of silver on bare and colloidal TiO_2 nanoparticles/nanotubes: synthesis, characterization, and tested for antibacterial outcome', *J. Phys. Chem. C*, 2007, **111**, pp. 13393–13397

[4] Shin J.-Y., Joo J.H., Samuelis D., Maier J.: 'Oxygen-deficient $TiO_{2-\delta}$ nanoparticles via hydrogen reduction for high rate capability lithium batteries', *Chem. Mater.*, 2012, **24**, pp. 543–551

[5] Musumeci A., Gosztola D., Schiller T., *ET AL.*: 'SERS of semiconducting nanoparticles (TiO_2 hybrid composites)', *J. Am. Chem. Soc.*, 2009, **131**, pp. 6040–6041

[6] Faure B., Lindelov J.S., Wahlberg M., Adkins N.: 'Spray drying of TiO_2 nanoparticles into redispersible granules', *Powder Technol.*, 2010, **203**, pp. 384–388

[7] Garnweitner G., Ghareeb H.O., Grote C.: 'Small-molecule in situ stabilization of TiO_2 nanoparticles for the facile preparation of stable colloidal dispersions', *Colloids Surf. A*, 2010, **372**, pp. 41–47

[8] Zhang S.Y., Yu Q.M., Li Y.L., Yang Y., Wang Q., Chen Z.H.: 'The effecting factors of super-dispersion TiO_2 nanoparticles prepared by sol-emulsion-gel method', *Rare Metal Mater. Eng.*, 2008, **37**, pp. 326–329

[9] Veronovski N., Andreozzi P., La Mesa C., Sfiligoj-Smole M.: 'Stable TiO_2 dispersions for nanocoating preparation', *Surf. Coating Technol.*, 2010, **204**, pp. 1445–1451

[10] Nakayama N., Hayashi T.: 'Preparation and characterization of poly (L-lactic acid)/TiO_2 nanoparticle nanocomposite films with high transparency and efficient photodegradability', *Polym. Degrad. Stab.*, 2007, **92**, pp. 1255–1264

[11] Luo Y.-B., Wang X.-L., Xu D.-Y., Wang Y.-Z.: 'Preparation and characterization of poly(L-lactic acid)-grafted TiO_2 nanoparticles with improved dispersions', *Appl. Surf. Sci.*, 2009, **255**, pp. 6795–6801

[12] Bensebaa F., Durand C., Aouadou A., *ET AL.*: 'A new green synthesis method of $CuInS_2$ and $CuInSe_2$ nanoparticles and their integration into thin films', *J. Nanopart. Res.*, 2010, **12**, pp. 1897–1903

[13] Kang S., Yin D., Li X., Li L., Mu J.: 'One-pot template-free preparation of mesoporous TiO_2 hollow spheres and their photocatalytic activity', *Mater. Res. Bull.*, 2012, **47**, pp. 3065–3069

[14] Rao Y., Antalek B., Minter J., *ET AL.*: 'Organic solvent-dispersed TiO_2 nanoparticle characterization', *Langmuir*, 2009, **25**, pp. 12713–12720

[15] Yu J., Zhao X., Du J., Chen W.: 'Preparation, microstructure and photocatalytic activity of the porous TiO_2 anatase coating by sol-gel processing', *J. Sol-Gel Sci. Technol.*, 2000, **17**, pp. 163–171

[16] Ghosh P.K., Maity R., Chattopadhyay K.K.: 'Electrical and optical properties of highly conducting CdO:F thin film deposited by sol-gel dip coating technique', *Sol. Energy Mater. Sol. Cells*, 2004, **81**, pp. 279–289

[17] Sun L., Zhao X., Cheng X., Sun H., Li Y., Li P., Fan W.: 'Synergistic effects in La/N codoped TiO_2 anatase (101) surface correlated with enhanced visible-light photocatalytic activity', *Langmuir*, 2012, **28**, pp. 5882–5891

[18] Lin H., Huang C.P., Li W., Ni C., Shah S.I., Tseng Y.-H.: 'Size dependency of nanocrystalline TiO_2 on its optical property and photocatalytic reactivity exemplified by 2-chlorophenol', *Appl. Catal. B*, 2006, **68**, pp. 1–11

[19] Kormann C., Bahnemann D.W., Hoffmann M.R.: 'Preparation and characterization of quantum-size titanium dioxide', *J. Phys. Chem.*, 1998, **92**, pp. 5196–5201

[20] Bocchini S., Fukushima K., Blasio A.D., Fina A., Frache A., Geobaldo F.: 'Polylactic acid and polylactic acid-based nanocomposites photooxidation', *Biomacromolecules*, 2010, **11**, pp. 2919–2926

[21] Chen Y.-K., Lin Y.-F., Peng Z.-W., Lin J.-L.: 'Transmission FT-IR study on the adsorption and reactions of lactic acid and poly(lactic acid) on TiO_2', *J. Phys. Chem. C*, 2010, **114**, pp. 17720–17727

[22] Achmad F., Yamane K., Quan S., Kokugan T.: 'Synthesis of polylactic acid by direct polycondensation under vacuum without catalysts, solvents and initiators', *Chem. Eng. J.*, 2009, **151**, pp. 342–350

[23] Bosch-Jimenez P., Lira-Cantu M., Domingo C., Ayllon J.A.: 'Solution processable TiO_2 nanoparticles capped with lauryl gallate', *Mater. Lett.*, 2012, **89**, pp. 296–298